Optics Communications 326 (2014) 114–120

Contents lists available at ScienceDirect

Optics Communications

journal homepage: www.elsevier.com/locate/optcom

Investigation of optical inhomogeneity of MgO:PPLN crystals for frequency doubling of 1560 nm laser

Shanlong Guo, Yulong Ge, Yashuai Han, Jun He, Junmin Wang *

State Key Laboratory of Quantum Optics and Quantum Optics Devices (Shanxi University), and Institute of Opto-Electronics, Shanxi University, No. 92 Wu Cheng Road, Tai Yuan 030006, Shan Xi Province, PR China

ARTICLE INFO

Article history:
Received 3 January 2014
Received in revised form
26 March 2014
Accepted 4 April 2014
Available online 24 April 2014

Keywords:
Second harmonic generation
1560 nm telecom laser
MgO:PPLN bulk crystal
Optical inhomogeneity

ABSTRACT

The asymmetrical phase-matching temperature tuning curves of periodically-poled 5%-mol MgO-doped lithium niobate (MgO:PPLN) bulk crystals for frequency doubling of 1560 nm telecom laser have been observed experimentally and analyzed theoretically. We find that the asymmetrical phenomena are resulted from the variation in the extraordinary refractive index by the doping concentration inhomogeneity of the crystals. The critical parameters of phase-matching temperature mismatching γ ($\gamma=\delta T_{pm}/\Delta T$, in which δT_{pm} is the change of the phase-matching temperature due to the doping concentration inhomogeneity, and ΔT is the temperature acceptance bandwidth) and the thermal refractive index $\partial(\Delta n)/\partial T$ are investigated. Our analysis method is not only a reasonable explanation to the experiment, but also can be a simple evaluation way of optical quality of the given MgO:PPLN bulk crystals. Moreover, the MgO:PPLN bulk crystal is used in single-pass configuration for frequency doubling a 4.4 W Erbium-doped fiber amplifier boosted 1560 nm telecom laser, and 300 mW of tunable 780 nm laser is obtained, corresponding to a conversion efficiency of 6.9%. This source provides a simple and compact laser system for rubidium atom cooling and manipulation experiments.

1. Introduction

Frequency doubling for the production of high power, high beam quality and high stability 780 nm laser radiation source has wide applications in the atomic physics over past several decades, such as the portable atom interferometry based sensors [1,2], cooling the rubidium-87 atom application in the space [3], ns pulse laser applied to the rubidium atom manipulation [4] and atomic frequency standard [5]. Owning to the great simplicity and stability, the single-pass frequency doubling configuration of quasi-phase-matching (QPM) crystal has been a good attractive approach to the above fields. Compared with the external cavity resonant enhancement technology, there is no complicated servo loop to stabilize the optical cavity actively [6], meanwhile, the telecom fiber components available of the fundamental wave can provide good stability. With the fast-developing area of master oscillator fiber power amplifier systems, the fundamental laser output power can be amplified up to dozens of watts, which is obviously helpful for high power second harmonic generation (SHG) for the single-pass configuration [7,8].

Vital in the attainment of practical powers and efficiencies in this configuration is the ability to utilize long interaction lengths and the highest nonlinear coefficient accessible in QPM materials. A QPM material candidate for SHG is periodically-poled $KTiOPO_4$ (PPKTP), offering moderate effective nonlinear coefficient ($d_{eff}\sim$ 10 pm/V), low thermal conductivity makes it more sensitive to thermal effects, limiting its use at higher powers [9]. Periodically-poled $LiTaO_3$ (PPLT) is also a potential material, which possesses higher thermal conductivity, and with an effective nonlinear coefficient ($d_{eff}\sim$9 pm/V) comparable to PPKTP, but its temperature acceptance bandwidth is narrower than PPKTP [10]. Another attractive QPM material candidate is periodically-poled lithium niobate (PPLN) crystals, which has been widely established for nonlinear frequency conversion applications, due to a mature fabrication technology, large effective nonlinearity ($d_{eff}\sim$16 pm/V), wider temperature acceptance, and widespread availability in interaction lengths up to 50 mm. However, its more extensive applications have been restricted by photorefractive effects and optical damage. Doping with MgO not only improves the ability of photorefractive resistance but also decreases the phase-matching temperature, however, whether the MgO doped in the PPLN crystal (MgO:PPLN) is homogeneous or not is really a technology challenge, it has been an important factor affecting SHG conversion efficiency [11], since the phase-matching temperature T_{pm} of the SHG is an extremely sensitive function to the stoichiometry

* Corresponding author.
E-mail address: wwjjmm@sxu.edu.cn (J. Wang).

http://dx.doi.org/10.1016/j.optcom.2014.04.008
0030-4018/

ratio of lithium (Li) to niobium (Nb) in the crystal [12], MgO doping concentration uniformly in the crystal will affect the stoichiometry ratio of Li/Nb, therefore, it is interesting to investigate the dependence of conversion efficiency on the non-uniformity of MgO doping concentration of MgO:PPLN crystals. Bortz et al. [13] reported the axial inhomogeneity in the PPLN waveguide by measuring wavelength tuning curves. Later, Helmfrid and Arvidsow [14] introduced a model that assumes the phase mismatch term consisting of a linear and a parabolic part to interpret the optical inhomogeneity in the QPM waveguide. Lee et al. [15] also simulated this kind of variation by the temperature gradient control technique in a periodically-poled Ti:$LiNbO_3$ waveguide. Our studies focus on this particular aspect of the inhomogeneity MgO:PPLN bulk crystal for frequency doubling of 1560 nm laser. In this context, a practical analyzing method can be adopted in experiment is the temperature dependence tuning curve, it can be a simple and effective evaluation method to identify homogeneity of MgO doping concentration for MgO:PPLN bulk crystals.

In our paper, we report and analyze the asymmetric multi-peak phase-matching temperature tuning properties of MgO:PPLN bulk crystals. Taking appropriate physical model (the single-step model and the multi-step model) to fit the experimental data well, we obtain two key physical parameters (the phase matching temperature mismatching $\gamma=\delta T_{pm}/\Delta T$, in which δT_{pm} is the change of the phase-matching temperature due to the doping concentration inhomogeneity and ΔT is the temperature acceptance bandwidth, and the thermal refractive index $\partial(\Delta n)/\partial T$) used to characterize the doping concentration inhomogeneous of the crystal. The analysis method is a quantitative method which is a general model used to evaluate doping concentration in arbitrary length QPM crystal. Additionally, two MgO:PPLN bulk crystals with relatively good symmetrical temperature tuning characteristic are used in single-pass configuration for frequency doubling of 1560 nm telecom laser. After a 4.4 W Erbium-doped fiber amplifier (EDFA) boosted 1560 nm telecom laser, we obtain 300 mW of 780 nm laser with a conversion of 6.9%.

2. Analysis of optical inhomogeneity of MgO:PPLN bulk crystals

2.1. Theoretical model for the optical inhomogeneity

The variation of the second harmonic (SH) power versus temperature (equivalent to an aperture plane wave) in an ideal crystal (i.e., no refractive index variation) should show a $[\sin(\Delta kl/2)/(\Delta kl/2)]^2$ dependence [16], however, if the doping concentration non-uniformly, there will appear a distortion with the $[\sin(\Delta kl/2)/(\Delta kl/2)]^2$ function to the temperature tuning curve. Here we assume that the non-ideal crystal is composed of several ideal regions along the X axis, each ideal region owns independent length, the phase-matching temperature and the extraordinary refractive index for the fundamental wave (and the SH wave).

Considering the optical inhomogeneity of the crystal, the SHG intensity can be described by the "single-step model" and the "multi-step model" [17]. Both theoretical models are characterized by a monotonic change and neglect the absorption of the laser in the crystals, such assumptions can be consistent with the observation in experiment and with the view of the asymmetric characteristic occurred in the course of doping MgO into a $LiNbO_3$ crystal from the melt. The "multi-step model" is the further extension of the "single-step model", it takes more regions dividing from the given crystal, owning more advantage and flexibility, so it can be adopted to more complicated issues of the asymmetrical temperature tuning curve of the non-ideal crystal.

2.1.1. The single-step model

For the periodically-poled nonlinear crystal whose total crystal length $l=l'+l''$. We assume that two regions l' and l'' divided from the crystal has different extraordinary refractive index for the fundamental wave (and the SH wave) along the X axis (the laser propagation direction) due to the doping concentration inhomogeneity, it will lead to the different phase mismatching Δk and the phase-matching temperatures of the SHG process for these two regions, however, the extraordinary refractive index for the fundamental (and the second harmonic) is the same in its own region(l′ or l″). Thus the SHG power P_2 emerging from the far end of the crystal can be summed over the radiation in the SHG electric field from each incremental volume [18]. It can be shown as:

$$P_2(M=1)\propto\{l'^2[\sin(\Delta k'l'/2)/(\Delta k'l'/2)]^2+l''^2[\sin(\Delta k''l''/2)/(\Delta k''l''/2)]^2 +2l'l''[\sin(\Delta k'l'/2)/(\Delta k'l'/2)][\sin(\Delta k''l''/2)/(\Delta k''l''/2)] \times\cos[(\Delta k'l'+\Delta k''l'')/2]\} \quad (1)$$

In appearance the formula (1) is two separate $[\sin(\Delta kl/2)/(\Delta kl/2)]^2$ functions for the two regions of the crystal plus a "beat" term. The M is the number of steps.

The Δk is the phase mismatching in the QPM, which is given by $\Delta k=\Delta k'-k_m$, the $k_m=2\pi m/\Lambda$ is the mth-harmonic grating wave vector, Λ is the QPM crystal grating period. In our experiment, $m=1$. The normal phase mismatching $\Delta k'=4\pi/\lambda_1\times(n_2^e-n_1^e)$, where n_2^e and n_1^e are the extraordinary refractive index in the crystal for the SHG and fundamental beams, respectively, λ_1 is the fundamental wavelength. Assuming that the phase mismatching Δk should be approximately a linear function of the temperature, so the Δk as a function of the crystal temperature T can be expanded in a Taylor series expansion at the phase-matching temperature T_{pm}

$$\Delta k=\frac{4\pi}{\lambda_1}\frac{\partial\Delta n}{\partial T}(T-T_{pm}) \quad (2)$$

where $\Delta n=(n^e{}_2-n^e{}_1)$, it denotes the difference of the extraordinary refractive index between the fundamental wave and the SH wave.

For a convenient calculation later, the variable substitution are adopted to the formula (1), then the "single-step" model to the normalized SHG power P_2 can be written as follows:

$$P_2(M=1)\propto\left\{\frac{\sigma^2}{(1+\sigma)^2}\left\{\frac{\sin[\sigma\varphi/(1+\sigma)]}{\sigma\varphi/(1+\sigma)}\right\}^2 +\frac{1}{(1+\sigma)^2}\left\{\frac{\sin[\varphi/(1+\sigma)+\beta\gamma/(1+\sigma)]}{\varphi/(1+\sigma)+\beta\gamma/(1+\sigma)}\right\}^2, +\frac{2\sigma}{(1+\sigma)^2}\left\{\frac{\sin[\sigma\varphi/(1+\sigma)]}{\sigma\varphi/(1+\sigma)}\right\} \times\left\{\frac{\sin[\varphi/(1+\sigma)+\beta\gamma/(1+\sigma)]}{\varphi/(1+\sigma)+\beta\gamma/(1+\sigma)}\right\}\cos\left(\varphi+\frac{\beta\gamma}{1+\sigma}\right)\right\} \quad (3)$$

where $\varphi=\Delta kl/2$ is the phase mismatching, $\sigma=l'/l''$ is the proportion of the two parts' lengths of the crystal, $\beta=\pi/1.125$, and $\gamma=\delta T_{pm}/\Delta T$. Here γ is the phase matched temperature mismatching, δT_{pm} is total change of the phase matched temperature along the X axis of the crystal, experimentally it will show the shift of the phase matched temperature major peak, and ΔT is the temperature acceptance bandwidth of the whole crystal length.

We assume that the T_{pm} is due solely to a variation of extraordinary refractive index between fundamental and SHG. It can be written as $\delta T_{pm}=-\delta(n_2^e-n_1^e)/[d(n_2^e-n_1^e)/dT]$, while the temperature acceptance bandwidth can be $\Delta T=\lambda_1/\{2.25l\times[d(n_2^e-n_1^e)/dT]\}$ (the detailed theoretical derivation process about δT_{pm} and ΔT can be seen in Appendix A). Then the ratio of these two variable quantity (γ) reflects the variation of the extraordinary refractive

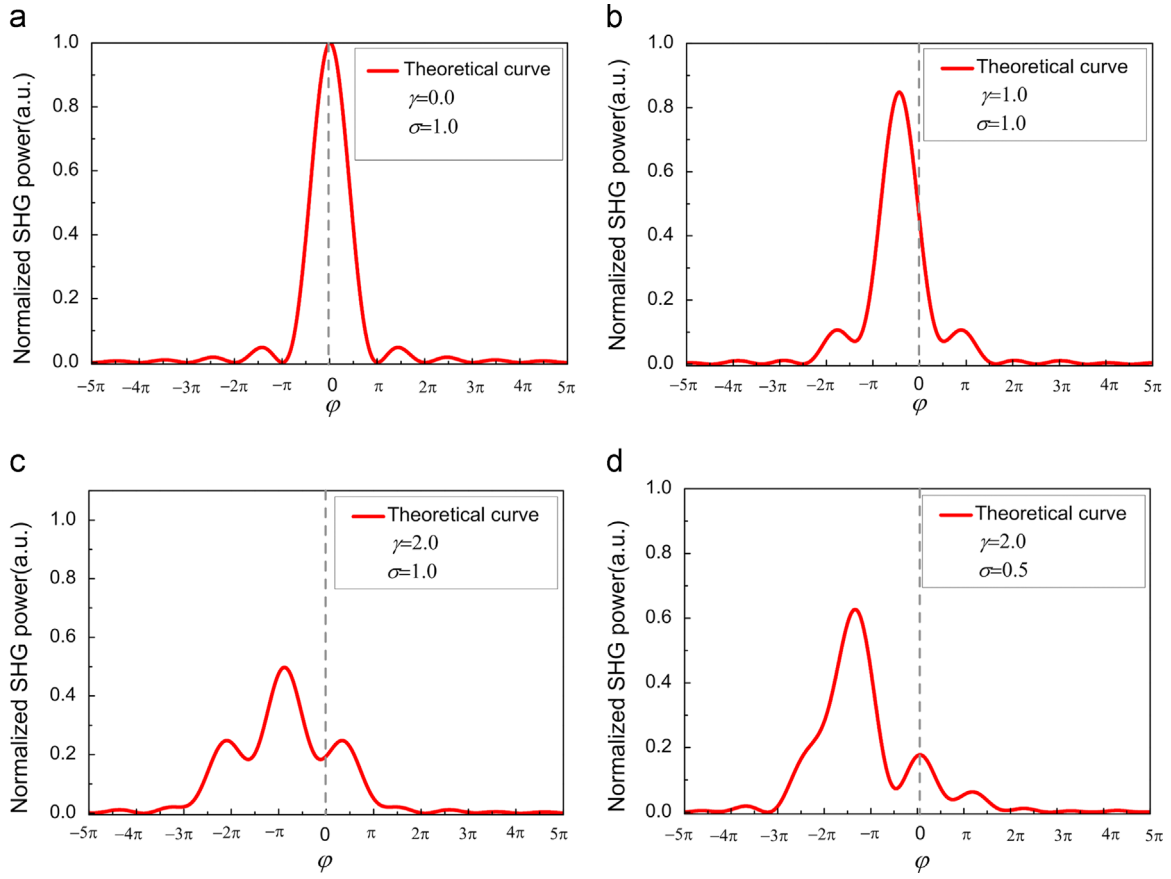

Fig. 1. The simulation calculations comparison of the normalized SHG power for the "single-step model" at $\gamma=0.0$ (a), $\gamma=1.0$ (b) with $l'=l''$ ($\sigma=1.0$) and the calculations at $\sigma=1.0$ (c), $\sigma=0.5$ (d) with $\gamma=2.0$.

index between the fundamental and the SHG precisely along the X axis.

As a quantization parameter, γ describes the degree of the temperature tuning asymmetrical distortion along the total crystal length exactly. When $\gamma=0.0$ (no index distortion) and $\sigma=1.0$ ($l'=l'$) represent the ideal temperature tuning behavior (Fig. 1 (a)), and the $\gamma=1.0$, 2.0 cases show an increasing symmetrical distortion ($\sigma=1.0$), the simulated calculation results in Fig. 1 (b) and (c). Experimentally one typically observes asymmetry in the side band structure of temperature tuning curve. Meanwhile, asymmetry distortion can be also introduced by the variation of the relative lengths of the two regions ($\sigma\neq 1$), such as the simulated calculation results of Fig. 1(c) and (d).

From the simulation results, it is can be deduced that different doping concentration regions of the crystal had rather different phase matched T_{pm} along the X axis; additionally, the ΔT is also different with different crystal lengths along the X axis [19]. An empirical criterion for adequate crystal quality might be given by $\delta T_{pm}\leq\Delta T$; however, if the δT_{pm} is larger more than the ΔT, it will state the doping concentration uneven more in the crystal.

2.1.2. The multi-step model

In practice, to the given crystal, only two regions divided from the crystal, often cannot truly reflect the doping concentration distribution in the samples, so there needs more meticulous dividing to make it approach the practical situation. If the crystal can be regarded as N regions ($N\geq 2$, similarly, we assume that each region is ideal doping without index distortion), one is able to use M steps ($M=N-1$) theory for the calculations. In this case, the lengths of all regions are considered to be equal (It means that $\sigma=1$ in any steps) and the M step heights are either equal. Supposing each part of the MgO:PPLN crystal along the X axis is phase matched at its own temperature, similar to the "single-step model", the normalized SHG power P_2 of the "multi-step model" can be expanded as:

$$P_2(M=N-1)\propto\left(\frac{l}{N}\right)^2\times\left(\sum_{n=1}^{N}A_n^2+2\sum_{s=1}^{N-1}\sum_{n=1}^{N-s}A_nA_{s+n}B_{sn}\right), \tag{4}$$

where

$$A_n=\frac{\sin\{\varphi/N+(n-1)\beta\gamma/N(N-1)\}}{\varphi/N+(n-1)\beta\gamma/N(N-1)}, \tag{5}$$

$$B_{sn}=\cos\left[2s\left(\frac{\varphi}{N}+\frac{(n-1+\frac{1}{2}s)\beta\gamma}{N(N-1)}\right)\right], \tag{6}$$

For $M=1$ ($N=2$), the "multi-step model" formula (4) reduces to "single-step model" formula (1) with $\sigma=1$, so the "single-step model" can be regarded as a special case to the "multi-step model". Since the "multi-step model" gives more regions divided from the crystal, it can reflect more complex shape of the temperature tuning curve, typically, we simulate the theoretical temperature tuning curves for 2, 3 and 4 regions of the crystal with different σ in Fig. 2(a) and (b).

2.2. Experimental results and analysis for the optical inhomogeneity

There are three samples of MgO:PPLN bulk crystals (HC Photonics Corp) with a nominal doping concentration of 5% mol in our hands. All the dimensions of the crystals are 1 mm × 3.4 mm × 25 mm parallel to the Z, Y, and X axis, containing a single grating

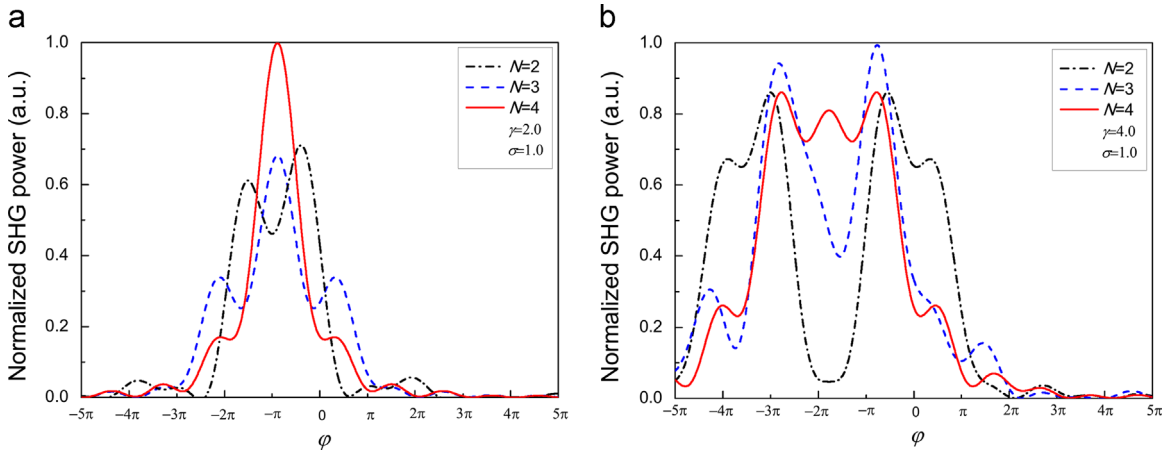

Fig. 2. The simulation calculations comparison of the normalized SHG power for the "multi-step model" (typically $N=2, 3, 4$) at $\gamma=2.0$, $\sigma=1.0$ (a) and at $\gamma=4.0$, $\sigma=1.0$ (b).

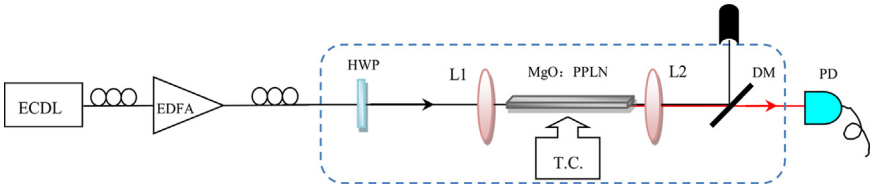

Fig. 3. Schematic of the single-pass frequency doubling experimental setup. ECDL: extended grating cavity diode laser; EDFA: Erbidum-doped fiber amplifier; HWP: half-wave plate; L1, L2: focus lens; T.C.: temperature controller; DM: dichroic mirror; PD: photodiode.

period of $\Lambda=19.48$ μm. The propagation of 1560 nm in the SHG experiment is all along the X direction, both the input and output sides of the crystals are AR coated for the 1560 nm and 780 nm. For convenience, three MgO:PPLN crystals are named as the crystal A, B and C.

The experimental setup used for single-pass SHG is shown schematically in Fig. 3. We used the 1560 nm tunable extended-grating-cavity diode laser (ECDL, New Focus TLB_6328) as the seed laser, power amplifying by a continuous-wave erbium-doped fiber amplifier (EDFA), producing the maximum output power up to ~5 W at 1560 nm. Frequency doubling by 25-mm-long MgO:PPLN crystal with the single-pass configuration, the focus lens L1 (focal length $f=50$ mm) is to focus the fundamental wave in order to increase the laser intensity in the crystal. Dichroic mirror is utilized to separate the SHG (transmissivity $T\sim98\%$ for 780 nm) from the fundamental wave (reflectivity $R\sim99.8\%$ for 1560 nm). The 780 nm laser's power is measured by a laser power meter (Coherent, Field Mate).

The QPM crystal is housed in a temperature controlled oven, which was made from red copper, the precision of the temperature controller (Newport Model 350B) is 0.01 °C. The accurate determination of the phase-matching temperature is a key to achieve optimum SHG conversion efficiency in the QPM crystal. We scanned the crystal temperature at a fixed fundamental power level with the single-pass configuration, the experiment data is shown in Fig. 4(a)–(c). The solid line and dash dot line are the fitted curve according to the theoretical model for the asymmetrical temperature tuning curve.

The optimum phase-matching temperature of the crystal A and B measured centered at ~81.4 °C, and centered at ~79.8 °C for the crystal C. The temperature acceptance bandwidth of the A and B crystal measured is ~3.8 °C and ~3.7 °C from the experimental results, respectively. The observed asymmetric temperature dependences of the MgO:PPLN samples in the experiment is deviating from the theoretically predicted $[\sin(\Delta kl/2)/(\Delta kl/2)]^2$ shape of Fig. 4(d) and the undoped PPLN crystal in our previous experiment [20]. Especially for the crystal C, it displays a more apparent asymmetric multi-peak dependency characteristic at the fixed fundamental power (500 mW), and the similar result has been obtained at the higher fundamental power experimentally (1 W fundamental power input). The SHG powers at the phase-matching temperatures of 73.5 °C and 79.8 °C for the crystal C, are both only half of that obtained at the optimum phase-matching temperature of the crystal A (81.4 °C) at the same fundamental power (500 mW), such temperature tuning characteristic of the crystal will be no doubt to reduce the conversion efficiency dramatically for our subsequent frequency doubling experiment.

A possible reason caused this asymmetric temperature tuning characteristic in the crystal is the imperfective crystal structure when the crystal is fabricated. Normally, the most likely non-ideal periodic structures to appear in a QPM crystal are the periodically-poled errors and the periodically-poled losses. However, due to the non-accumulative characteristic of the periodically-poled errors, no change in the width of the sinc^2 function shape is observed, but rather only a reduction by a certain proportion; and it is a similar effect for the periodically-poled losses [21]. Another possible reason we should attention is that the phase-matching temperature T_{pm} is an extremely sensitive function of stoichiometry ratio of Li to Nb, if MgO doped into the crystal is non-uniform, it will cause the uneven distribution of Li ion and Nb ion in the wafer, further inducing the variation of phase-matching temperature T_{pm} of the MgO:PPLN crystal.

According to the theoretical model of the asymmetric temperature tuning curve, the parameter of phase matched temperature mismatching γ determines the height ratio of sideband to the main peak and the horizontal moving of the whole curve, the bigger of the γ, and the bigger of the height ratio of the sideband to the main peak, and the whole curve is moving gradually to low temperature region, and when the N is bigger, these two trends are more prominent, both the γ and N determine the shape of curve. Simulating different regions divided of the crystals, we find the experiment results are consistent with the $N=6$, $N=2$, and $N=7$

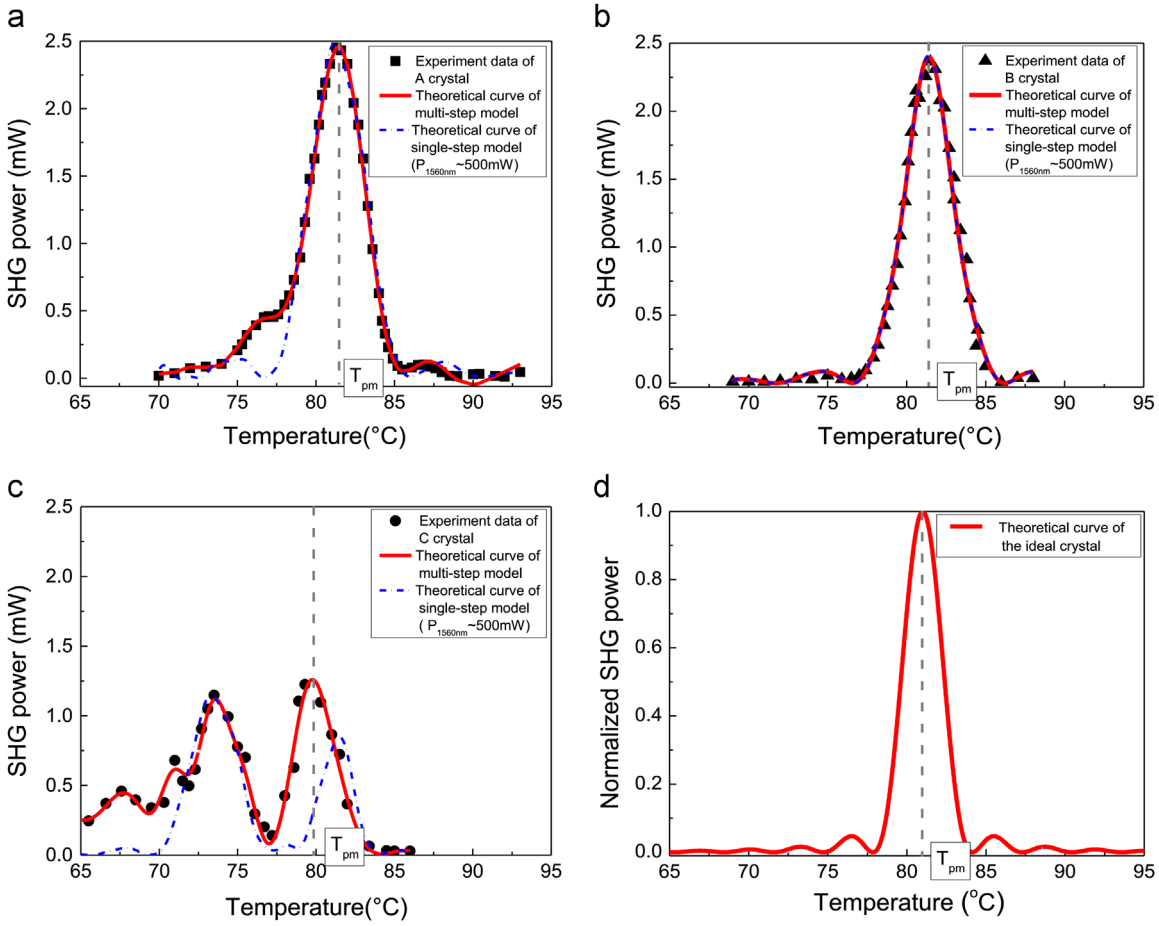

Fig. 4. Temperature tuning characteristic of crystals A (a), B (b) and C (c). Dots are experimental data, the solid lines are the theoretically fitted curves using "multi-step model", the short dash dot lines are the theoretically fitted curves using "single-step model". (d) is the theoretically predicted temperature tuning curve of ideal crystal. T_{pm} is the optimum phase-matching temperature of the crystal.

Table 1
Fitting parameters of the "single-step model" and the "multi-step model".

MgO:PPLN samples	Single-step model				Multi-step model			
	N	σ	γ	$\partial(\Delta n)/\partial T$ ($\times 10^{-5}$/°C)	N	σ	γ	$\partial(\Delta n)/\partial T$ ($\times 10^{-5}$/°C)
Crystal A	2	1.51	5.70	1.98	6	1.00	1.85	1.49
Crystal B	2	1.00	9.70	3.60	2	1.00	9.70	3.60
Crystal C	2	0.59	7.96	1.81	7	1.00	1.62	3.39

for the crystal A, B and C, respectively, further optimizing the fitting parameters of γ for three crystals, we obtained the good fitting results as Fig. 4, and the fitting parameters are presented in Table 1. According to the optical inhomogeneity theory model, the fitted curves we obtained show reasonably good agreement with the experiment data, and the thermal refractive index $\partial(\Delta n)/\partial T$ are close to the reported literature value (1.6×10^{-5}/°C) [22]. It is proved that the theoretical model is suitable for the experiment phenomena. Additionally, the "single-step model" is also used to fit the experiment data, however, the fitting results of the crystal A and C are not as good as the "multi-step model". It indicates that the "single-step model" cannot fully describe more asymmetric temperature tuning curves as desirable compared with the "multi-step model". We note that the absolute peak intensity does vary with the change in different fundamental power levels, but we are concerned here with the falloff from ideal behavior of $[\sin(\Delta kl/2)/(\Delta kl/2)]^2$ function due to the introduction of the distortion. So the present theoretical model does not consider absorption at the fundamental or second harmonic wavelengths. Various focusing conditions and various fundamental power levels have been tested in SHG scan and we observed no clear influence to the distortion, the absorption of the two waves in the crystals is so trivial [23] that we can neglect the influence of the thermal effect to the experiment results. Therefore, the theoretical model is valid for low power where the absorption effects are insignificant and it is not possible to decouple thermal effects with doping inhomogeneity effects while operating at high power levels.

Normally, congruent $LiNbO_3$ crystals are grown by the conventional Czochralski method with a typical nonstoichiometric composition (Li/Nb=48.6/51.4), which will generate Li defects [24]. According to the viewpoint of Ref. [17], the phase-matching temperature distortion resulted from stoichiometric variations of the Li/Nb ratio which occurred during pulling for the birefringent bulk crystal; However, to the MgO:PPLN crystal which is prepared

by the vapor transport equilibration (VTE) technology in our experiment, the reason is rather caused by the uneven doping concentration. For VTE preparation technology, it is firstly taking the 5% mol. MgO:PPLN wafer with Li ion diffusion in the Li-rich surrounding for a long time (> 100 h) [25], the intent is to increases the Li content of the wafer to achieve the homogenization of the Li, Nb and MgO in the crystal finally. However, if the doped MgO distributed non-uniformly in the wafer, it will replace the Li ion and Nb ion on different levels in crystal lattice during the Li exchange process, at last, there will induce the inhomogeneous optical characteristics for the different regions of the crystal. In Ref. [11], the researchers get the number of the regions of the waveguide being divided but no more quantitative information about the asymmetric distribution of waveguide, in our work we further get the explicit physics meaning parameter of phase matched temperature mismatching γ and the thermal refractive index $\partial(\Delta n)/\partial T$, these two physical parameter can quantify the degrees of the doping concentration inhomogeneity of the crystal.

Although different regions which are divided in the crystal had rather different T_{pm} and the different $\partial(\Delta n)/\partial T$, but their locations in the crystal are hardly known precisely, therefore we can just obtain the total variation of the T_{pm} along the whole crystal length. Due to the imperfection of the crystal doping concentration inhomogeneity occurred in the melt when the crystal is fabricated, once the chip is finished, it cannot be modified easily for the experimenters.

3. Frequency doubling results and analysis

It has been found due to the optical inhomogeneity the SHG conversion efficiency was decreased by shortening the effective phase-matching length, here we take crystals A and B which show the relative good temperature tuning feature of the three samples as QPM crystal in experiment, measuring the frequency doubling conversion characteristic. The single crystal SHG was characterized by using of plano-convex lens L1 (f=50 mm, in Fig. 3) to focus fundamental beam at the center of the MgO:PPLN crystal to a waist radius w=35 μm, which is close to the optimum focusing for SHG [26]. Using a single crystal in the single-pass configuration, we get 303 mW (301 mW for B crystal) 780 nm laser for a fundamental power of 4350 mW (4360 mW for crystal B) at a conversion efficiency of 6.9%. These results are shown in Fig. 5, the squares and the dots are the experimental data for crystal A and B, respectively. The solid line is the theoretical calculation curve of the SHG power generated by the focused Gaussian beams

$$P_2 = \frac{8\pi \times d_{eff}^2}{n_1^2 n_2 \lambda_1^2 c\varepsilon_0} \times P_1^2 \times l \times k_1 \times h_m(\sigma_m, B, \zeta)\,, \tag{7}$$

where the k_1 is the wave-vector of the fundamental, the dimensionless function h_m is called Boyd–Kleinman (BK) factor, which is given in Ref. [26]

$$h_m(\sigma_m, B, \zeta) = \frac{1}{4\zeta}\left(\int_{-\zeta}^{\zeta} d\tau \frac{\cos(\sigma\tau)+\tau\,\sin(\sigma\tau)}{1+\tau^2}\right)^2, \tag{8}$$

The confocal length $z = l/b(b = 2\mathrm{p}w^2/l), \tau = 2(z-f)/b$, where z is the observation point along the laser propagation direction, f is the focal position in the crystal, the optimum phase mismatch parameter σ_m is obtained by changing the crystal temperature experimentally, the optimum focusing function h_m=1.068, which is found for ζ = 2.84 (to the QPM crystal, there is no walk-off effect between the fundamental wave and the SH wave, so the B=0).

Analyzing the deviation between our experiment and the theoretical calculation, one main reason is absorption of the crystal to the SH wave and thermal dephasing effect between the fundamental and the SH waves in the experiment, since the formula (8) neglects absorption of the crystal to the fundamental and the SH waves, and consider both the waves are in the perfective phase matching case. And the other reason is the imperfective focus waist. For the optimum waist radius is ~32 μm according to the BK factor, while the factual waist radius is ~35 μm which is measured by the knife blade. Therefore, the situation will be more obvious with the absorption increases in the higher fundamental power region (particularly when fundamental power exceeds 3.5 W in experiment).

Limited by the crystal length and fundamental power level, the reported experimental result is the maximum output power we were able to achieve at the present time. If the input power for the fundamental is higher [7] or longer length crystal can be adopted [27], there will be a higher achievable SHG power output.

In order to characteriz the 780 nm laser beam quality obtained by the single-pass frequency doubling, we used a charge coupled device (CCD) camera to measure the transverse intensity profile of the laser beam (after passing through a neutral density filter), and a typical result is provided as the inset of Fig. 5 with Gaussian fitting in the horizontal and vertical directions. The 780 nm laser beam's quality factor is measured as M^2 ~1.07 by the knife blade method.

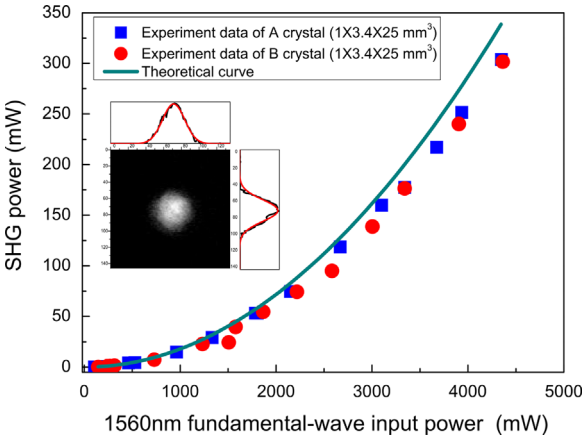

Fig. 5. Dependence of the SH output power on the fundamental power for single-pass frequency doubling (squares for the crystal A, dots for the crystal B and the solid line is the theoretical curve). The inset is the transverse intensity profile of the 780 nm laser beam measured by a CCD camera.

4. Conclusions

In conclusion, asymmetric variations in the phase-matching temperature for SHG using the bulk MgO:PPLN crystal have been observed in experiment. We attribute this phenomenon to the variations in the extraordinary index of refraction caused by changes in the doped crystal stoichiometry occurring in the growth process. The optical inhomogeneity theory provides a good fit to the experimental data and provides the extraordinary index of refraction at different temperatures of the MgO:PPLN crystals. The explanation can also be a quality test to the uniformity of doping concentration in a periodically-poled bulk crystal. Furthermore, we present a generation system of the 780 nm cw laser with single-pass frequency doubling configurations. The 780 nm laser power of 300 mW with conversion efficiencies of 6.9% is obtained at an operating temperature (~81 °C). This frequency-doubling laser system can be used for laser cooling and manipulation of rubidium atoms.

Acknowledgments

This project is supported by the National Major Scientific Research Program of China (Grant No. 2012CB921601), the National Natural Science Foundation of China (Grant Nos. 11274213, 61205215, and 61227902), the Project for Excellent Research Team from the National Natural Science Foundation of China (Grant No. 61121064), the Shanxi Scholarship Council of China (Gran No. 2012-015), and Program for Science and Technology Star of Taiyuan, Shanxi, China (Grant No.12024707).

Appendix A

For the given MgO:PPLN crystal, the temperature acceptance bandwidth ΔT and the variations in T_{pm} along the X axis (the beam propagation direction), the mathematics derivation process are present below.

The refractive index at the phase-matching temperature T_{pm} for quasi-phase-matched SHG in terms of the index at a nearby temperature T can be represented by a Taylor series expansion

$$(n_2^e - n_1^e)_{T_{pm}} = (n_2^e - n_1^e)_T + (T_{pm} - T) \times d(n_2^e - n_1^e)/dT\,, \tag{A1}$$

The momentum mismatching of the SHG is (we assume Λ is the grating period of the QPM crystal)

$$2 \times k_1 - k_2 - \frac{2 \times \pi}{\Lambda} = \Delta k\,, \tag{A2}$$

And it can also be written as:

$$\frac{4 \times \pi}{\lambda_1} \times (n_1^e - n_2^e)_T - \frac{2 \times \pi}{\Lambda} = \Delta k\,, \tag{A3}$$

so

$$(n_1^e - n_2^e)_T = \frac{\lambda_1 \times \left(\Delta k + \frac{2 \times \pi}{\Lambda}\right)}{4 \times \pi}\,, \tag{A4}$$

when the phase matching condition is achieved, the$\Delta k = 0$, the formula (4) can be read

$$(n_1^e - n_2^e)_{T_{pm}} = \frac{\lambda_1}{2 \times \Lambda}\,, \tag{A5}$$

so the formula (1) can be described

$$T_{pm} - T = \frac{-\frac{\lambda_1}{2\Lambda} - (n_2^e - n_1^e)_T}{d(n_2^e - n_1^e)/dT}\,, \tag{A6}$$

Take the formula (3) into the (5), there will be

$$T_{pm} - T = \frac{-\frac{\lambda_1}{2\Lambda} + \frac{\left(\Delta k + \frac{2\pi}{\Lambda}\right) \times \lambda_1}{4\pi}}{d(n_2^e - n_1^e)/dT}\,, \tag{A7}$$

For the ideal crystal (the crystal length is l) the second harmonic power versus temperature should show a $[\sin(\Delta kl/2)/(\Delta kl/2)]^2$ dependence, the function will fall to a half, when $\Delta kl/2 = \pi/2.25$,

Thus, the temperature acceptance bandwidth

$$\Delta T = \frac{\lambda_1}{2.25l \times d(n_2^e - n_1^e)/dT}\,, \tag{A8}$$

Now in considering variations in T_{pm} along the propagation direction, if we assume that any variation in T_{pm} is due solely to a change in extraordinary refractive index for the fundamental n_1^e and SHG n_2^e, so we go back to (5) and replace T by T_r (room temperature, it is set as a constant), then

$$\delta T_{pm} = -\delta(n_2^e - n_1^e)/d(n_2^e - n_1^e)/dT \tag{A9}$$

References

[1] F. Lienhart, S. Boussen, O. Carat, N. Zahzam, Y. Bidel, A. Bresson, Appl. Phys. B 89 (2007) 177.
[2] V. Menoret, R. Geiger, G. Stern, N. Zahzam, B. Battelier, A. Bresson, A. Landragin, P. Bouyer, Opt. Lett. 36 (2011) 4128.
[3] F. Lienhart, S. Boussen, O. Carraz, N. Zahzam, Y. Bidel, A. Bresson, Appl. Phys. B 89 (2007) 177.
[4] J. Dingjan, B. Darquie, J. Beugnon, M.P.A. Jones, S. Bergamini, G. Messin, A. Browaeys, P. Grangier, Appl. Phys. B 82 (2006) 47.
[5] V. Mahal, A. Arie, A. Mark, M.M.Fejer Arbore, Opt. Lett. 21 (1996) 1217.
[6] J.X. Feng, Y.M. Li, Q. Liu, J.L. Liu, K.S. Zhang, Appl. Opt. 46 (2007) 3593.
[7] M.Y. Vyatkin, A.G. Dronov, M.A. Chernikov, D.V. Gapontsev, V.P. Gapontsev, Proc. SPIE 5709 (2005) 125.
[8] S.W. Chiow, T. Kovachy, J.M. Hogan, M.A. Kasevich, Opt. Lett. 37 (2012) 3861.
[9] G.K. Samanta, S.C. Kumar, M Mathew, C. Canalias, V. Pasiskevicius, F. Laurell, M. Ebrahim-Zadeh, Opt. Lett. 33 (2008) 2955.
[10] S.C. Kumar, G.K. Samanta, M. Ebrahim-Zadeh, Opt. Express 17 (2009) 13711.
[11] H.L. Jiang, G.H. Li, X.Y. Xu, Opt. Express 17 (2009) 16073.
[12] J.G. Bergmann, A. Ahskin, A.A. Ballman, J.M. Dziedzic, H.J. Levinstein, R.G. Smith, Appl. Phys. Lett. 12 (1968) 92.
[13] M.L. Bortz, S.J. Field, M.M. Fejer, D.W. Nam, R.G. Waarts, D.F. Welch, IEEE J. Quantum Electron. 30 (1994) 2953.
[14] S. Helmfrid, G. Arvidsson, J. Opt. Soc. Am. B: Opt. Phys. 8 (1991) 797.
[15] Y.L. Lee, Y.C. Noh, C. Jung, T.J. Yu, B.A. Yu, J. Lee, D.K. Ko, K. Oh, Appl. Phys. Lett. 86 (2005) 011104.
[16] P.A. Franken, J.F. Ward, Rev. Mod. Phys. 35 (1963) 23.
[17] F.R. Nash, G.D. Boyd, M. Sargent, P.M. Bridenbaugh, J. Appl. Phys. 41 (1970) 2564.
[18] G.D. Boyd, A. Ashkin, J.M. Dziedzic, D.A. Kleinman, Phys. Rev 137 (1965) 1305.
[19] G.D. Boyd, W.L. Bond, H.L. Carter, J. Appl. Phys. 38 (1967) 1941.
[20] S.L. Guo, Y.S. Han, J Wang, B.D. Yang, J. He, J.M. Wang, Acta Opt. Sin. 32 (2012) 0319001 (in Chinese).
[21] M.M. Fejer, G.A. Magel, D.H. Jundt, R.L. Byer, IEEE J. Quantum Electron. 28 (1992) 2631.
[22] O. Gayer, Z. Sacks, E. Galun, A. Arie, Appl. Phys. B 91 (2008) 343.
[23] J.R. Schwesyg, M.C.C. Kajiyama, M. Falk, D.H. Jundt, K. Buse, M.M. Fejer, Appl. Phys. B 100 (2010) 109.
[24] J.R. Carruthers, G.E. Peterson, M. Grasso, J. Appl. Phys. 42 (1971) 1846.
[25] Y. Furukawa, K. Kitamura, S. Takekawa, A. Miyamoto, M. Terao, N. Suda, Appl. Phys. Lett. 77 (2000) 2494.
[26] G.D. Boyd, D.A. Kleinman, J. Appl. Phys. 39 (1968) 3597.
[27] R.J. Thompson, M. Tu, D.C. Aveline, N. Lundblad, L. Maleki, Opt. Express 11 (2003) 1709.